Photovoltaic-Electrolyzer (PV-EC) System Operated at >50mA/cm^2 by Combining Large Area Shingled Silicon PV Module with High Surface Area Nickel Electrodes for Low-cost Green H_2 Generation

*Nina Plankensteiner *, Amedeo Agosti, Jonathan Govaerts, Rico Rupp, Sukhvinder Singh, Jef Poortmans, Philippe M. Vereecken, Joachim John**

Nina Plankensteiner
Imec, Energy Department, Kapeldreef 75, 3001 Leuven, Belgium
KULeuven, cMACS, Celestijnenlaan 200F, 3001 Leuven, Belgium
nina.plankensteiner@imec.be

Amedeo Agosti, Jonathan Govaerts, Rico Rupp, Sukhvinder Singh
Imec, Energy Department, Kapeldreef 75, 3001 Leuven, Belgium

Jef Poortmans
Imec, Energy Department, Kapeldreef 75, 3001 Leuven, Belgium
KU Leuven, Department of Electrical Engineering, Kasteelpark Arenberg 10, 3001 Leuven

Philippe M. Vereecken
Imec, Energy Department, Kapeldreef 75, 3001 Leuven, Belgium
KULeuven, cMACS, Celestijnenlaan 200F, 3001 Leuven, Belgium

Joachim John
Imec, Energy Department, Kapeldreef 75, 3001 Leuven, Belgium
joachim.john@imec.be

Keywords: solar fuels, low-cost green hydrogen, PV-EC system, shingled silicon PV, anion-exchange membrane water electrolysis, water splitting, high surface area electrodes

Green hydrogen will play an important role in the energy transition as a renewable energy vector for long-duration energy storage and as feedstock chemical for the industry. To reduce the price below 1.5 €/ kg H_2, competitive to production from fossil fuels, silicon PV-powered efficient anion exchange membrane (AEM) water electrolysis is a promising combination. Practical implementation of such a PV-EC technology requires standard area-sized solar cells and electrolyzers operated at large current densities. Nonetheless, state-of-the-art research often employs <10cm^2 PV devices and electrolyzers operated at current densities <10mA/cm^2. This article presents a commercially relevant PV-EC system that combines shingled standard silicon technology with an efficient and low-cost AEM electrolyzer based on high surface area (26m^2/cm^3) nickel nanomesh electrodes. The produced H_2, operating current & voltage were in-situ monitored over >20h. As such, the system constantly yields a stable solar-to-hydrogen efficiency (η_{STH}) of 10% at electrolyzer current densities ~60mA/cm^2 and dynamic load testing up to 300mA/cm^2 results in stable performance. Based on the measured PV-EC system data best practices to accurately determine the η_{STH} for PV-powered water splitting devices and the validation of this benchmark against important component parameters for practical implementation of this technology are discussed.

Table of contents entry

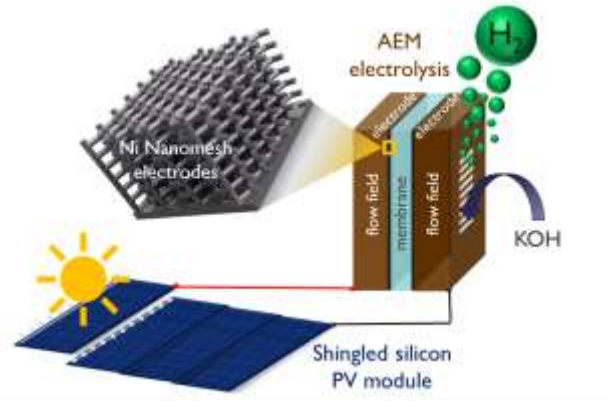

This work presents a PV-EC system combining shingled standard-sized silicon PV and anion-exchange membrane water electrolysis with high surface area electrodes. During >20h operation the system provides a stable η_{STH} of 10% determined through in-situ monitoring of the H_2 flow, operating

current/voltage. Best practices for the η_{STH} determination are discussed and referenced towards important parameters for practical device implementation.

1. Introduction

Limiting climate change by reducing global CO_2 emissions is one of the central challenges of the 21st century. This requires a profound restructuring of our energy systems and a far-reaching conversion to innovative and emission-free technologies in all sectors. Renewables combined with hydrogen as energy carrier can make a significant contribution to achieving climate protection goals in the medium to long term. While the cost of renewable energy generation technology continues to decrease, the costs to accommodate the growing proportion of renewable electricity in the distribution grid is growing, due the need for balancing services, grid expansion and the curtailment of surplus renewable electricity production. [1] Flexible consumers such as decentralized electrolyzers that can absorb the fluctuating renewable energies (FRE) help to reduce these costs. As such the German Advisory Council on the Environment (SRU) [2] points out that a decentralized location within Germany is crucial in order to ensure grid-friendly interaction with the electricity grid and allow suitable sector coupling. To this end, the technological and regulatory foundations must be laid with the aim of gradually establishing stand-alone green hydrogen technologies.

Based on the most recent solar energy auction with electricity costs as low as 0.013 $/kWh [3] and state-of-the-art electrolyzer system efficiencies of ~55-60 kWh/kgH_2 [4], a prospected Levelised-Cost-Of-Hydrogen (LCOH) of 1-1.5 €/kg H_2 can be expected already by 2030. These costs are competitive with grey H_2 generated from fossil fuels 1.5-3€/kg H_2 even without considering CO_2 taxation.[5] Such technological figures-of-merit have been recently backed by policy actions, such as the European Hydrogen Strategy [5] and the US Department of Energy Hydrogen Shot [6] initiatives.

For the generation of green hydrogen using solar energy three different technologies are commonly distinguished: Photo-electrochemical (PEC), photo-catalytic (PC) and coupled PV-EC systems. Among these technologies, the coupled PV-EC systems exhibit at this moment the highest technological readiness level and deliver the highest solar-to-hydrogen efficiencies (η_{STH}) [7,8]. In PV-EC systems the photovoltaic technology of choice, that commercially delivers low-cost electricity with stable efficiencies of 20-25% at 30-40mA/cm^2, [9] are in-series connected silicon solar cells, providing >1.23V for water splitting. In the next decade, silicon-tandem configurations with perovskite top-cells might play an additional role with conversion efficiencies approaching 30%.

[10,11] The electrical efficiency of water electrolysis varies between 50-70%$_{LHV}$ for the classical alkaline electrolysis and up to 80%$_{LHV}$ at current densities up to 2A/cm^2 for the most efficient, but costly polymer electrolyte membrane electrolysis (PEM). [12] The most promising new improvement in the water electrolysis field are the alkaline anion exchange membrane electrolyzers (AEMs) that combine the high performance of PEM with low-cost materials and components used in alkaline electrolysis. High electrical efficiencies up to >75%$_{LHV}$ operated at >2A/cm^2 or even higher are predicted in the next 20-30 years.[12,13] At academic level, although major improvements for the individual PV-EC components were demonstrated, expensive niche photovoltaic technologies, such as III-V multijunction small area CPV devices [14–16] and classical alkaline or expensive PEM electrolysis systems, operated at low current densities <0.01A/cm^2, are often utilized.[15] Notable exceptions are shown in the PECSYS project, in which large-area silicon devices were implemented for the first time in a PV-EC system [17,18] and the work by Schüttauf et al., in which small PV devices are combined with PEM electrolysis operating at ~50mA/cm^2.[19]

In this article, a PV-EC system in a commercially relevant configuration is presented as an important step towards low-cost green hydrogen. We combine shingled, in-series connected state-of-the-art large-area silicon solar cells with a zero-gap AEM electrolyzer including high surface area (26m^2/cm^3) earth-abundant nickel nanomesh electrodes. In-series shingling of silicon solar cells is an especially attractive approach for solar water splitting applications, since a sufficient high voltage per standard cell area can be achieved. The high potential of using nickel nanomesh electrodes for alkaline water electrolysis was demonstrated in our previous work [20–22]. It was shown that nanomesh electrodes significantly outperform state-of-the-art nickel foams (0.001-0.008m^2/cm^3) due to their high surface area and accessibility of active catalytic sites for water electrolysis [23,24]. Important operating parameters such as H_2/O_2 yield, current and voltage of the PV-EC system were continuously in-situ measured via a custom-built monitoring that is coupled between PV and electrolyzer component. Based on the data obtained we discuss best practices to determine the solar-to-hydrogen (STH) efficiency and propose a way to benchmark this figure of merit against state-of-the-art solar-based water splitting.

2. Results and Discussion

2.1. Anion-exchange membrane electrolyzer

The lab-scale single-cell electrolyzer used in this work contains two 4µm thin high-surface area nickel nanomesh electrodes (more details in our previous work) [22] pressed against a commercial anion-exchange membrane in a zero-gap architecture as shown in the schematic in **Figure 1(a).** 1M KOH is circulated as electrolyte at 30˚C in the commercial single-cell electrolyzer (see **Figure 1(b)**). A pre-conditioning step of the electrolyzer (10min, 100mA/cm^2) is required to guarantee a stable operation prior to the PV-EC experiments. During the pre-conditioning the electrodes are stabilized in their proper oxidation state according to their catalytic activity, the membrane is activated for the OH^- transport [25–28] and the circulated electrolyte is pre-saturated with H_2 and O_2 to avoid dissolution of products in the initial electrolysis phase. The as-assembled stack yields at 100mA/cm^2 a cell voltage of 2.29V and a high ohmic resistance of 8.2 Ohm*cm^2 as shown in the current density vs. cell voltage plots in **Figure 1(c)** and the Impedance Nyquist plots in **Figure 1(d)**. After the pre-conditioning the ohmic resistance decreases to 2.4 Ohm*cm^2 and the cell voltage decreases by 100mV at 100mA/cm^2.

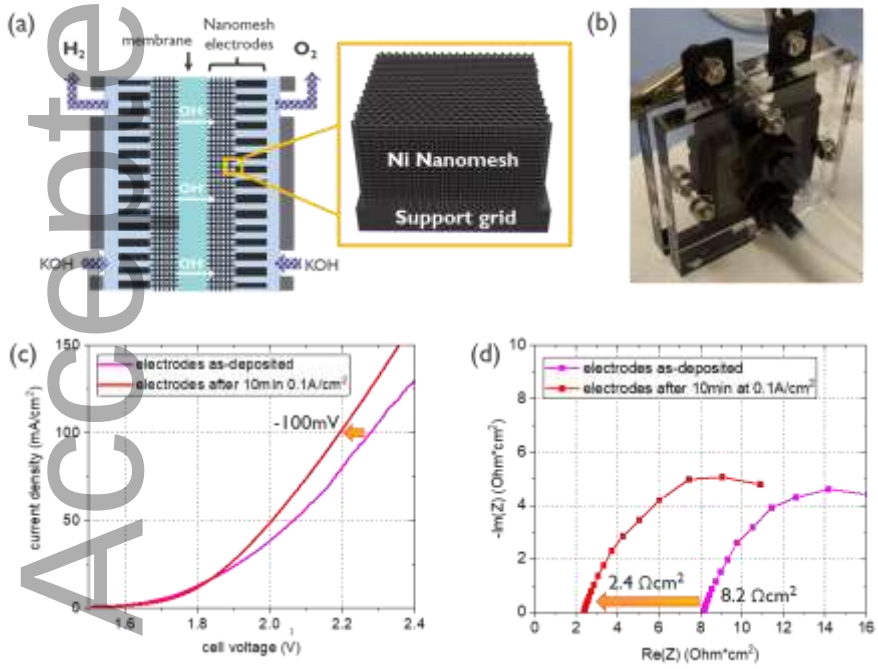

Figure 1 *(a) Schematic of single-cell electrolyzer with nickel nanomesh electrodes, (b) image of the electrolyzer, (c) current density vs. voltage curve for the AEM electrolyzer with 1M KOH at 30˚C with/without pre-conditioning, (d) EIS Nyquist plots showing the ohmic resistance with/without pre-conditioning of the electrolyzer*

2.2. Shingled silicon PV minimodule

A PV module consisting of 6 silicon heterojunction cells (shingles of 38.5cm^2 cut from 15.6x15.6cm^2 standard cells) assembled into a string using a shingling strategy was fabricated. The cells were connected in-series and span a variable open-circuit voltage range from 0.7V to 4.3V, depending on the number of cells connected as shown in **Figure 2(a)-(c)**. Under standard testing conditions using a solar simulator at 1 sun, the different IV-curves with a constant short-circuit current (I_{sc}) of 1.42 A (or 36.9mA/cm^2, single cell area 38.5cm^2) are recorded as shown in **Figure 2(c)** and **Table 1**. A stable cell efficiency of ~20% was determined on all cell configurations with fill factors close to 80%. The current-voltage characteristics from the electrolyzer showed that 1.8 – 2.2V are required to match an electrolyzer current density between 20 and 100mA/cm^2. This minimum voltage requirement can be achieved by connecting 3 or 4 silicon cells in-series.

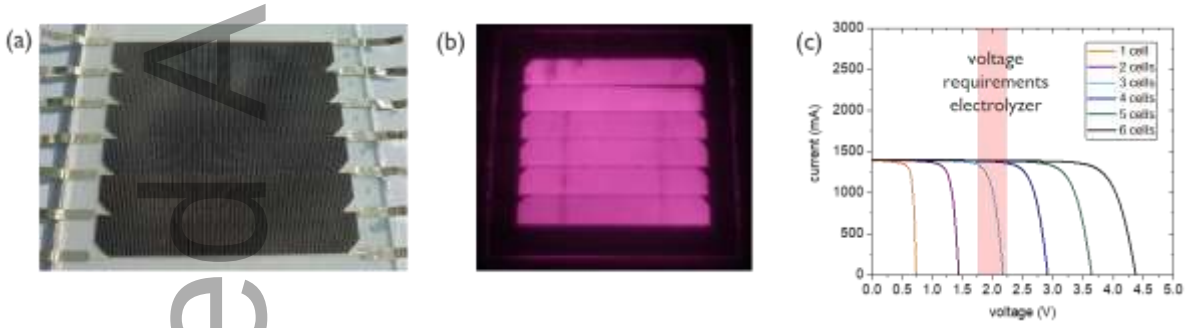

Figure 2*(a) Image of shingled silicon module with 1-6 cells connected in-series, (b) electroluminescence image of the silicon module (c) IV curves of 1-6 silicon solar cells connected in-series under 1.5g illumination in a solar simulator*

Table 1: *Solar cell characteristics of 1 up to 6 cells connected in-series*

Number of cells	Area (cm^2)	T (°C)	Efficiency (%)	I_{sc} (A)	J_{sc} (mA/cm²)	V_{oc} (V)	FF (%)
1	38.5	25.14	20.8	1.45	37.7	0.73	79.4
2	38.5	26.62	19.6	1.42	36.9	1.44	77.6
3	38.5	26.63	19.9	1.42	36.9	2.17	78.4
4	38.5	25.95	20.0	1.42	36.9	2.92	78.3
5	38.5	25.92	20.0	1.42	36.9	3.64	78.2
6	38.5	25.81	20.2	1.43	37.1	4.37	78.7

2.3. PV-EC system under operation

To optimize the amount of H_2 generated from a PV-EC system several aspects have to be considered, such as initial matching of the maximum power point voltage (V_{MPP}) of the PV module with the operating potential (V_{OP}) required for electrolysis, decrease of cabling or peripheral component losses and long-term stability of the individual/combined components. As shown in **Figure 2(c),** the minimum voltage requirement for water splitting is fulfilled by a minimum of 3 in-series connected solar cells, with 4 cells providing an improved matching with the IV characteristic of the electrolyzer. The V_{OP} of combining 3 vs. 4 cells with the electrolyzer were determined with 1.85V and 2.45V, respectively, as shown in **Figure 2(c)** under AM1.5g spectrum illumination. Note that all PV-EC experiments were done under constant lab-scale illumination by a halogen lamp at 733 W/m^2 (determined from calibration against 1.5g spectrum, halogen lamp spectrum shown in SI) resulting in slightly lower currents and voltages (see **Figure 3(a))**. Under both illumination sources, the V_{MPP} of 4 cells matches best with the electrolyzer and under lab-scale illumination 2.3W is provided by the PV minimodule. The theoretical operating point (OP) of the combined PV-EC setup is determined with ~2.1V at ~1A as shown in **Figure 3(b)**. Using 4 PV cells, the PV-EC system can be operated at slightly lower voltages than the V_{MPP} of the PV component, which will result in the most efficient solar energy to hydrogen conversion.[29] Connecting 5 or 6 cells would deliver the same current with the surplus power remaining unutilized for electrolysis.

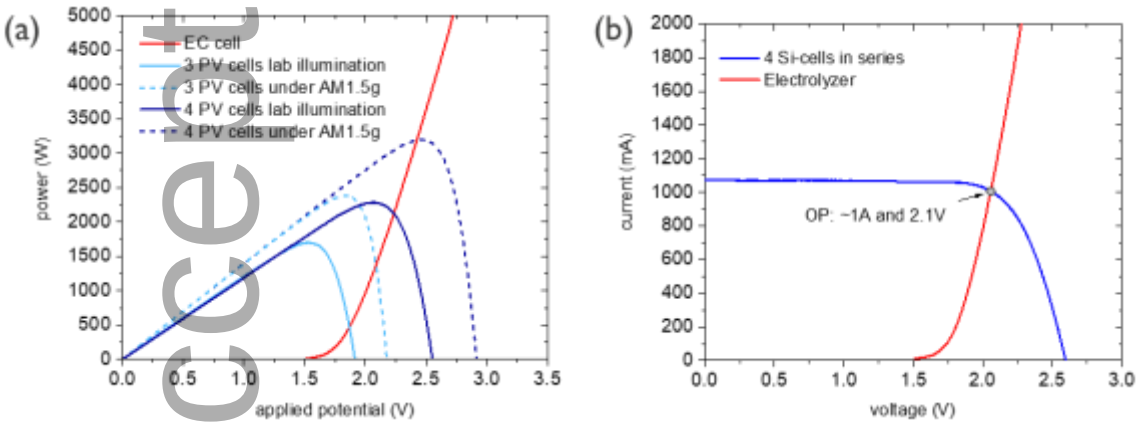

Figure 3 *(a) Matching PV and electrolyzer characteristics (PV module illuminated under AM 1.5g and halogen lab lamp) (b) theoretical operating point (OP) of 4 silicon PV cells connected to the electrolyzer (PV illuminated with halogen lamp)*

Based on the theoretical considerations and measurements of the individual components, 4 PV cells were directly connected to anode and cathode of the AEM electrolyzer via the PV-EC monitoring unit as shown in **Figure 4(a).** The monitoring unit simultaneously tracks the electrolyser H_2 and O_2 yield, as well as operating current and voltage. Rigorously quantifying these parameters to determine the efficiency of a (photo)electrochemical devices is of paramount importance for both fundamental

and applied research and allows us to obtain the η_{STH} of the system that is commonly used as figure-of-merit to compare devices.

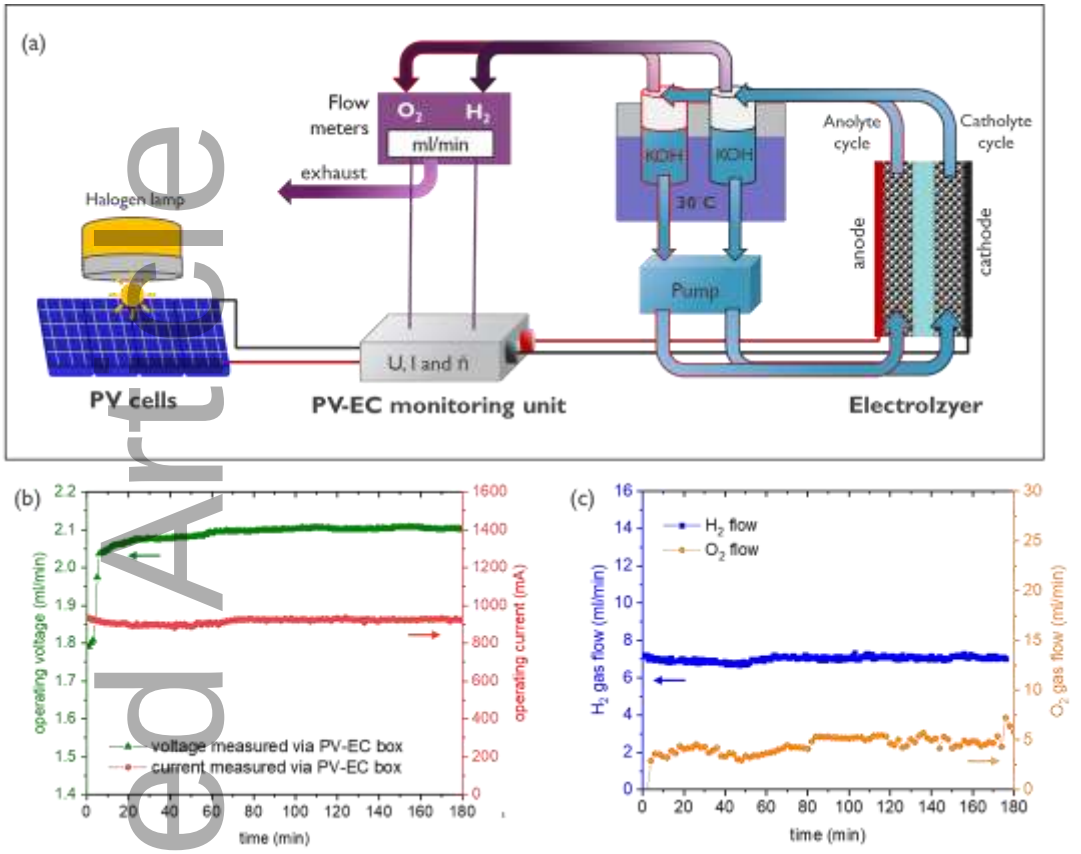

Figure 4 *(a) Schematic overview of the PV-EC system monitored by the PV-EC monitoring unit, (b(c)) 3h PV-EC operation monitoring (b) operating voltage and current and, (c) H_2 and O_2 flow*

The PV-EC system was initially operated under constant illumination with the halogen lab lamp (more information in SI) for a period of 3h and gaseous product flows, operating current and voltage were continuously in-situ monitored as shown in **Figure 4(b)(c)**. Within the first 5 minutes of connecting the PV and electrolyzer components, a voltage of 2.04V and a current of 917mA were recorded, stabilizing to 2.1V and 925mA after ~60min. The initial significant variation in voltage in the first 5 minutes from 1.79 to 2.04 V could be explained by minor changes in the electrolyzer characteristics referring to the necessary pre-conditioning of the nickel electrodes and the membrane. After the 3h experiment a slight shift of the electrolyzer IV-curve to lower overpotentials together with lower ohmic resistance was observed (see SI) confirming the slight changes at the electrolyzer component. In addition, it is possible that in the first measurement hour a stable temperature at the PV minimodule is not yet reached, causing a slight decrease of the V_{OC} of the PV module and therefore a shift of the optimum system V_{OP} counteracting the possible cell voltage change at the electrolyzer. Overall, the measured PV-EC operating voltage and current corresponds well with the

individual device characteristics (see **Figure 3(b)**), taking into account the ~2% losses from the integration of the PV-EC monitoring unit and cabling losses (see SI). The PV-EC system produces H_2 with a constant flow of 7.1ml/min and 3-4ml/min O_2 over the 3h period with the expected product ratio of ~2:1. The observed instabilities of the O_2 flow are caused by the flow meter. The produced gas amounts result in ~99% Faraday efficiency and a H_2 production rate of 2.23 g/h*m^2 taking into account the total PV area of 154cm^2. The determined system parameters between 60-180min of operation are summarized in **Table 2**.

Table 2: PV-EC system operating characteristics between 60 and 180min

Voltage (V)	2.10 +/-0.01
Current (mA)	924.95 +/- 2.96
Current density at Electrolyzer (mA/cm^2)	57.81
H_2 flow (ml/min)	7.07 +/- 0.08
FE (%)	98.83 +/- 2.79
H_2 production rate (g/h*m^2)	2.23

*All presented values are averaged between 60-180min of operation. Standard deviations were calculated considering the accuracy of the electronic components and measurement deviations.

2.4. Determination of the 'Solar-to-hydrogen efficiency' η_{STH}

The mostly used figure of merit to determine the efficiency of a PV-EC system is η_{STH}, a value that quantifies how much solar energy is converted to hydrogen fuel energy. The η_{STH} takes the whole system (PV module, electrolyzer, wiring, converters) into account and is typically calculated by considering either (1) the operating current, (2) the amount of produced H_2 or (3) the individual PV and electrolyzer component efficiencies combined with the coupling efficiency as shown by the three formulas in **Table 3**. Since in this work the H_2 flow and operating current/voltage are continuously in-situ monitored the η_{STH} can be determined over the whole operation time using all three formulas. In **Table 3** the η_{STH} was calculated taking the average parameters during the stable PV-EC operation between 60 and 180min of operation.

Table 3 *η_{STH} calculation formula and constants/values used for the calculation*

(1) from operating current	(2) from hydrogen flow	(3) EC/PV individual

$\frac{I_{OP}\ (A)\ * 1.23\ V\ * \eta_{FE}}{A_{PV}\ (m^2) * G_{photo}\ (W/m^2)}$	$\frac{\dot{n}H_2(mol/s)\ * LHV\ (\frac{J}{mol})}{A_{PV}\ (m^2) * G_{photo}\ (W/m^2)}$	$\eta_{EL} * \eta_{PV} * \eta_{coupling} * \eta_{FE}$
9.98%	**10.01%**	**10.07%**

I_{OP} (A) = 0.925A, V_{OP} = 2.10V, H_2 flow = 7.1 ml/min

LHV lower heating value of hydrogen = 237.2 kJ/mol

A_{PV}(m^2) = solar collection area = 0.00385m^2 *4 = 0.0154m^2

G_{photo} = irradiance (W/m^2) = 733 W/m^2 (lab illumination)

η_{FE} = 99% under PV-EC operation

$\eta_{EL\ (LHV)}$ = 1.23V/V_{OP} = 59.7% (theoretical operating voltage from **Figure 3(b)**)

η_{PV} = 20.0% (determined under STC)

$\eta_{coupling}$ = (I_{OP} * V_{OP})/P_{MPP}=85.20%

The most reliable way to calculate the η_{STH} is measuring the amount of H_2 produced (ideally in combination with gas purity measurements) and to constantly monitor the PV-EC operating current (formula (1) or (2)). It is essential for formula (1) and (3) to determine the Faraday efficiency (η_{FE}) from the generated H_2 gas volume to exclude other eventually occurring parasitic electrochemical reactions on the electrodes. In formula (3) the electrical efficiency of the electrolyzer and the PV efficiency are measured individually and $\eta_{coupling}$ is determined with 85.2% from the deviation of operating current/voltage from the MPP of the PV module. In literature $\eta_{coupling}$ is typically determined by using I_{OP}) and V_{OP} at the theoretical operation point of the superposed individually measured PV and electrolyzer IV-curves. Since I_{OP} and V_{OP} of this work are directly in-situ measured, an accurate $\eta_{coupling}$ of the whole PV-EC system (including peripheral losses) over the operation time can be determined resulting in a slightly higher η_{STH} compared to the calculations from the formulas (1) and (2). Overall, a stable η_{STH} of ~10% was reached for our PV-EC system.

2.5. Benchmarking of the η_{STH} to state-of-the-art

In industry, electrolyzers are typically operated at high current densities (>400mA/cm^2)[4,13] and solar cells are large area devices with standard cell sizes of 15.6x15.6cm^2 (~30-40mA/cm^2 for silicon-based devices).[9,30] Therefore, our goal was to cross-check these industrial constraints with current research on commercially relevant PV-EC systems and benchmark our PV-EC system with a η_{STH} of 10% against available literature. For the PV power source, silicon solar cells cover >92% of the current global PV market, providing low-cost electricity, and are therefore the most relevant technology. For the electrolyzer, all three low-temperature technologies, the classical alkaline, polymer-membrane and the emerging alkaline-membrane water electrolysis, are considered. As discussed in the previous section η_{STH} is the most common figure of merit reported to compare PV-EC systems. However, when taking into account the two important individual component parameters, such as the electrolyzer current density and the illuminated solar cell area, the reported η_{STH} are significantly below the best reported values >15%. [14–16]

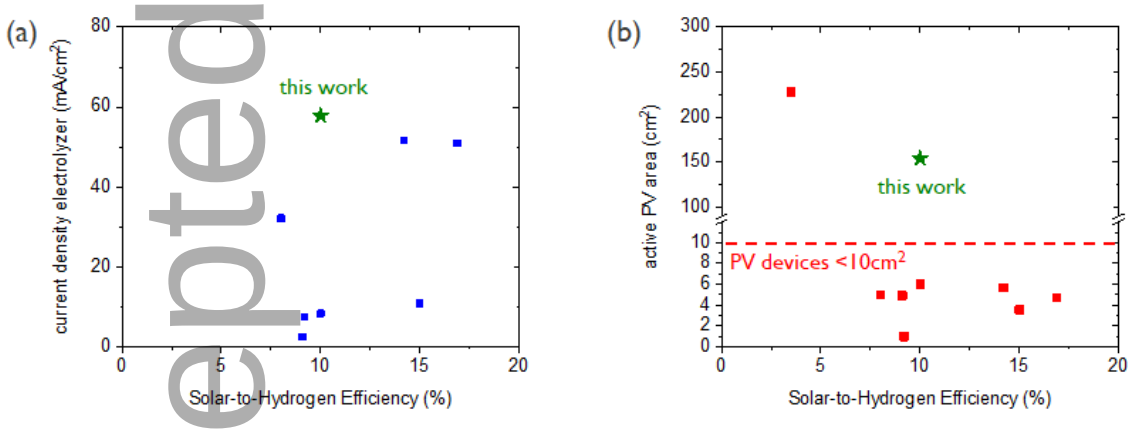

Figure 5 *Benchmarking of the silicon powered electrolyzer of this work against state-of-the-art PV-EC systems (including silicon PV and all low-temperature electrolysis technologies) (a) ηSTH and current density at electrolyzer relation* [19,31–36]*, (b)* η_{STH} *and active PV area relation* [17,19,31–36]

Figure 5(a) shows the electrolyzer current density values for PV-EC systems reported in literature plotted against the η_{STH}. The operating current density presented in this work is with ~60mA/cm^2 up to now the highest reported value in literature and stable performance at this current density was demonstrated. Unfortunately, this important parameter is often overlooked from the PV-EC research community and systems are mostly operated at <10mA/cm^2.[31,33,34] At such low current densities and low amount of H_2 produced, electrolyzer degradation (electrodes, membranes) is expected to be rather low. Although some of these systems were tested for long-term stability up to a few days [31,37], testing at low operating current densities has limited relevance for commercial applications.

In practice, the goal is to maximize the amount of H_2 produced and therefore testing these systems at higher operating current densities is vital towards practical implementation at a larger scale. Notable exceptions are the articles by Schüttauf [19] and Li et al. [32] that report stabilities up to 100h of their PV-EC systems at >30mA/cm^2.

In **Figure 5(b)** the active area of the silicon solar cells is compared against the reported η_{STH}. It is observed that most PV-EC systems operate with active solar cell areas <10cm^2, [19,31–36,38] which might be interesting for lab studies, but does not comply with industrial cell fabrication standards. The silicon solar cells used in this work were fabricated using the state-of-the-art shingling approach with standard cell sizes (active area of 154cm^2) and are apart from Schüttauf et al. [19] the largest silicon cells used in PV-EC systems reported in literature.

To summarize, although the η_{STH} is the standard reference value in literature to directly compare different PV-EC or even PEC and PC systems with each other, the findings above highlight the need to validate η_{STH} against the actual electrolyzer current density and active illuminated solar cell area, especially in regard to practical implementation of solar fuels. Next to setting the η_{STH} in respect to these important individual component parameters, the correct determination of the η_{STH} is of outmost importance. As proposed in this work a versatile monitoring unit with gas flow meters together with gas purity analysis via gas chromatography to exclude membrane gas-crossover can be used to access the faraday efficiency or directly use the gas flow rate for the η_{STH} determination with the formulas listed in **Table 3**. In literature the highest η_{STH} values for solar fuels are reported for PV-EC systems that use III-V multijunction small area CPV devices. In view of the ambitious goals for green hydrogen generation (EU 2030 40GW) the upscaling of III-V based CPV technology towards high volume production and cost of 1-1.5€/kg remains challenging.

2.6. PV-EC system >20h operation

To demonstrate that a stable high amount of H_2 can be produced for longer time periods, the PV-EC system was operated for 20h directly after the 3h experiment. **Figure 6(a)** shows the H_2 flow and operating current with values averaged over 30min intervals. A similar high H_2 production rate of 2.35 g/h*m^2 with a stable flow rate of 7.47 ml/min was observed yielding a Faraday efficiency close to 100%. The H_2 gas purity was determined with gas chromatography and a crossover of only ~1% O_2 was observed (details given in SI). The system operates at a stable average current of ~937mA (**Figure 6(a)**) with a voltage of 2.13V. Using formula (2) in **Table 2** we calculated the average η_{STH}

with 10% over 20h PV-EC and average $\eta_{coupling}$ with 85% (see **Figure 6(b)**). Both values remain stable over 20h with some improvements seen for the coupling efficiency to a maximum of 90% in the first 4h of operation and the maximum STH obtained together with the increased H_2 flow seen after 15h of operation. These results confirm that neither the PV nor the electrolyzer suffer from significant performance losses during the 20h measurement. To verify the stability of the electrolyzer we measured the electrolyzer IV curve after the 20h experiment and obtained a stable performance with a constant ohmic resistance (see SI).

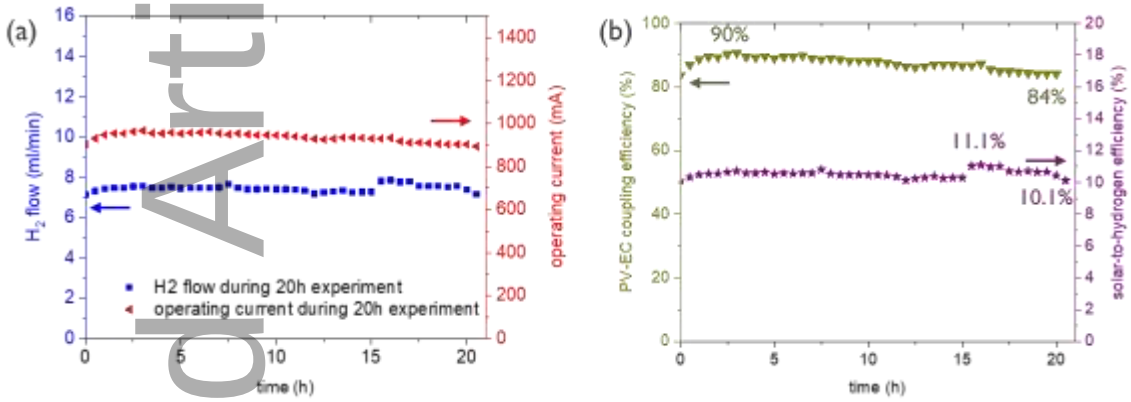

Figure 6: *PV-EC operation >20h (a) Monitoring of H_2 flow and current (b) PV-EC coupling and solar-to-hydrogen efficiency*

2.7. Dynamic load testing of the AEM electrolyzer

A major application of decentralized electrolyzers is to absorb the fluctuating renewable energies and to reduce the costs associated with equipping the electricity distribution grid. To assess the performance of electrolyzers under close to real-world dynamic conditions several testing protocols are proposed in literature.[39–42] Note, testing a single-cell electrolyzer under dynamic load profiles can provide some valuable information on intermittent operation and degradation factors however, a cell stack under real operation conditions needs balance of plant components that additionally influence the load profile.

To investigate the effect of a gradual and sudden increase in the applied load on the AEM electrolyzer with nickel electrodes two different experiments with a potentiostat as power input source were performed. It was shown that a cyclic triangle-wave operation (steady increase and decrease of the cell voltage) results in a similar loss pathway as the fluctuating solar power input over a solar day.[40]

In **Figure 7(a)** the current density of the electrolyzer over 180 solar cycles (~ half a year of solar days) up to a cell potential of 2.1V is shown. A decrease in the maximum current density at 2.1V of ~9% from 318 to 284mA/cm^2 is observed. This might be partly due to the required longer pre-conditioning period as observed by the voltage increase in the first hour of PV-EC operation. Additionally, at this testing conditions ~6 times higher current densities compared to the PV-EC operation at 60mA/cm^2 to demonstrate the capabilities of our electrolyzer under stressed conditions were applied. 180 continuous solar cycles translate at 60mA/cm^2 to a ~70mV increased cell voltage (**see Figure 7(b)**). As seen in **Figure 7(c)** the minor shift in the cell voltage has solely a limited influence on the operation point of the PV-EC system and therefore a similar high η_{STH} under the fluctuating solar radiation instead of constant lab illumination can be expected.

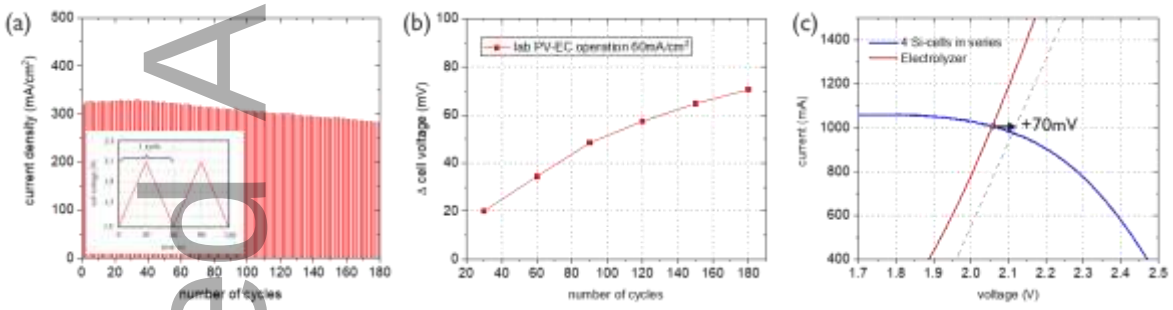

Figure 7: *(a) Current density in respect to the number of solar cylces with the inset showing the cycling conditions (b)cell voltage difference depending on the number of solar cycles at 60mA/cm^2 (c) effect of the cell voltage difference at 60mA/cm^2 (+70mV) on the operating point of the PV-EC system*

To assess the cell voltage response time of the AEM electrolyzer with sudden changes in the power input, a stepwise current profile according to the EU harmonized testing protocol was applied[39] consisting of 6 repeating sequence cycles starting with a nominal 100% current density of 0.1A/cm^2 and current steps 75, 50, 25% and open circuit voltage as shown in **Figure 8**. Small changes in the current density between 100 and 50% (that are larger than typical solar radiation fluctuations based on weather forecasts even on cloudy days [43]) result in a very quick response time of a few seconds to reach the initial cell voltage and increases to ~30s if switched between 25 and 100% current density. However, complete power shutdown of the electrolyzer results in a slower cell voltage response of roughly 1 min to reach the initial cell voltage at maximum current density. A similar shut on/off behavior is seen over all 6 sequence cycles. Overall, 6 test cycles result in 40mV increased total cell voltage from 1.85V to 1.89V demonstrating that the amount of tested abrupt changes in current densities and on/off times have a limited effect on the overall PV-EC performance of our system. Under real solar-operation conditions the downtime during the night has to be taken into account and

especially for nickel electrodes in the classical alkaline electrolysis this has shown to increase the overpotential for the electrochemical reaction at the electrodes due to the return to their original chemical state during shutdown.[43,44] To counteract this effect further development in electrode stability will be necessary that go beyond the scope of the present study.

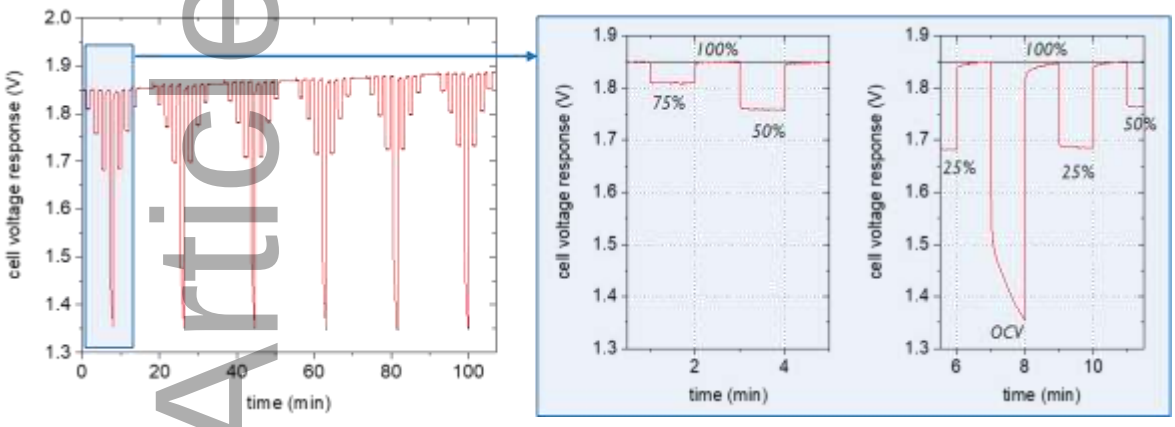

Figure 8: *(a) Cell voltage response during stepwise change in current density up to a maximum of 0.1A/cm2 (steps of 75, 50, 25% and OCV) with corresponding cell voltage, zoom-in on the cell voltage response of the first current step sequence*

3. Conclusion

In conclusion, we have combined large area solar devices with water electrolysis, operating at high current densities to produce a significant amount of H_2. Within this work, the usage of standard-sized solar cell technologies and the long-term electrolyzer stability at >50mA/cm^2 in respect to the electrode area under fluctuating power inputs were identified as requirements towards practical implementation of low-cost green hydrogen production from solar energy. The shown PV-EC system combines standard large-area silicon PV module shingling technology with next-generation high efficiency AEM electrolysis, using earth-abundant high surface area nickel electrodes. Stable performance of the PV-EC system during operation at 57.8mA/cm^2 over >20h with a η_{STH} of 10% was shown by in-situ monitoring of important system parameters, such as H_2 gas flow, current and voltage. To assess the effect of the fluctuating nature of solar energy input on the AEM electrolyzer performance dynamic load tests with gradual and abrupt power input changes over half a year of solar radiation results only in minor cell voltage changes and negligible impact on the PV-EC operation and H_2 production. Based on obtained measurement data during the PV-EC operation best practices for determination of the η_{STH} as important benchmark parameter for solar fuel systems are discussed.

Lastly, we highlight the importance to reference this figure-of-merit to the electrolyzer current density and the active solar cell area when moving from lab-scale towards practical relevant systems.

The next steps towards commercialization of the presented PV-EC system are long-term outdoor stability testing along with longer dynamic load measurement protocols. With the application of tandem-silicon modules (30% efficiency), decreased coupling losses to 5% through monolithic integration and/or additional thermo-management and catalytic coatings on the nanomesh electrodes, thus enhanced electrolyzer efficiency towards 85%$_{LHV}$, η_{STH} efficiencies close to 25% will be reachable within this decade.

4. Experimental Section

4.1. Lab-scale anion-exchange membrane electrolyzer

A zero-gap single-cell electrolyzer (H-TEC Education) that accommodates two porous nanomesh electrodes (4x4cm^2) and an ion-exchange membrane (4.5x4.5cm^2) pressed between two perforated stainless-steel grid plates was used (see **Figure 1(a)**). The stainless-steel grids, that act as current collectors, are in direct contact with the electrodes, have mm sized holes to allow the continuous electrolyte transport for the electrocatalytic reactions and the collection of the formed products H_2 and O_2. As cathode and anode, two 4µm thin freestanding nickel nanomesh electrodes with 70% porosity (26m^2/cm^3) and an 5µm open nickel support grid with 15% porosity as in detail described in our previous publication are applied (see **Figure 1(a)**).[20–22] Two 0.9mm Ni foams (NI00-FA-000140 Goodfellow) facilitate the contact between the steel grids and the nanomesh electrodes and a commercial membrane from Fumatech (Fumasep FAA PK-130) functioned as anion-exchange membrane. The membrane was immersed for at least 24h in 1M KOH (Potassium hydroxide solution 50%, VWR International, ELCH50488893) prior use. The 1M KOH as electrolyte was circulated with a dual-channel peristaltic pump (Ismatec Miniflex Digital Dual-Channel Pump) in a separated anolyte and catholyte cycle with flow rates of 20ml/min. The electrolyte temperature was kept at 30˚C by placing the electrolyte bottles in a water bath (Branson, CPX2800H, without sonication) as displayed in the PV-EC setup in **Figure 4(a)**. The products were collected above the circulated electrolyte in 100ml gas bottles with a direct gas outlet connected to H_2 and O_2 flow meters (Aalborg GFM17A-VBL6-A0 calibrated for H_2 and O_2). The flow rates were automatically read-out via the PV-EC monitoring unit as described below.

The IV-curve of the electrolyzer was recorded by linear sweep voltammetry (LSV) between 1.5 and 3V at 5mV/s on a Biologic VSP Multichannel potentiostat/galvanostat with EIS module connected to a 20A Biologic booster. Prior to the LSV, galvano electrochemical impedance measurement (GEIS) from 10kHz to 1Hz with 6 points per decade at 100mA and an amplitude of 10mA was recorded.

4.2. Shingled silicon PV minimodule

To provide potentials >1.23V plus the required overpotential for water splitting, a PV minimodule was fabricated within the framework of the H2020 Project HighLite [45]. The minimodule consists of 6 silicon heterojunction cells (shingles of 38.5cm^2 cut from 15.6x15.6cm^2 standard cells) assembled into a string using a shingling strategy and a metal ribbon in-between 2 neighboring cells (see images in **Figure 2**). This configuration allows to choose different voltage inputs for the electrolyzer. The string is embedded through a standard PV lamination cycle using a polyolefin encapsulant and glass on both sides as protection. Characterization of the minimodule is done on a LOANA measurement system, where a Xenon flash is used to calibrate the short-circuit current (I_{SC}), which is then used for calibrating the LED flash used for IV tracing to determine the IV-curve and obtain the I_{SC}, open-circuit voltage (V_{OC}) and fill factor (FF).

4.3. PV-EC system

Figure 4(a) schematically shows the setup of the PV-EC system, whereas the PV mini-module is interfaced to the electrolyzer via a custom-built PV-EC monitoring unit. Within this work the multi-purpose control unit was solely used to monitor the gas flows, current and voltage without the use of the integrated DC/DC converter. Briefly, the unit is composed by an Arduino board, managing data acquisition and logging, and voltage, current and mass flow meters sensors; the box also provides banana-sockets as interfaces for the power supply - a PV cell or a potentiostat - and the load, i.e. the electrochemical device. The PV-EC monitoring unit was built with inexpensive components and programmed with an open-source software, the whole project manual and code being available on Git-Hub. More details on the technical components including electrical losses are given in the supporting information.

During the PV-EC operation the PV module was illuminated with a halogen lamp (ELRO HL400S, 500W, positioned 30cm from the PV cells). The measured spectral response of the lamp is shown in

Figure S1 in the SI in comparison to the 1.5g standard spectrum. The G_{photo} of 733W/m^2 from the halogen lamp was obtained through normalization of the IV-curve of the lab illumination to the data obtained from LOANA measurements. Prior to connection to the electrolyzer, IV-curves of the PV modules under the lab illumination were recorded on a Biologic VSP Multichannel potentiostat/galvanostat (scan rate of 5mV/s). The solar cells were illuminated 30min prior the IV-recording to obtain stable lamp light spectrum and temperature on the module for the PV-EC measurements. The electrolyzer was operated at 30˚C with 1M KOH at a flow rate of 20ml/min, recirculated anolyte and catholyte separately.

4.4. Dynamic load testing of the electrolyzer

As electrolyzer setup the zero-gap assembly and components as described in our previous work were used [22] with the same nickel nanomesh electrodes and membrane as in section 4.1. To simulate the effect of the gradual increase of the solar energy over a day of illumination on the AEM electrolyzer a triangle-shaped increase and decrease of the cell potential from 1.5 till 2.1V with a rate of 20mV/s (60s for 1 cycle) was applied via a Biologic BCS-815 cycler. In-between 30 cycles an IV-curve from 1.5 till 2.1V with 5mV/s scan rate was measured to track the changes in cell voltage over cycling time. The stepwise decrease and increase in current density was done starting from a nominal maximum 100% current density at 0.1A/cm^2 followed by current steps of 1 min at 75, 100, 50, 100, 25, 100, OCV, 100, 25, 100, 50, 100, 75 and 100% current density for 1 testing cycle. The cycle sequence was repeated 6 times and an IV-curve from 1.5 till 2.0V with 5mV/s was measured in-between cycles to track the changes in the cell voltage over cycling time.

Supporting Information

Supporting Information is available from the Wiley Online Library or from the author.

Conflicts of Interest

No conflicts of interest to declare.

Acknowledgements

This work has been financed by the PROCURA project ("Power to X and Carbon Capture & Utilization Roadmap for Belgium") funded by the FOD Economy (K.M.O., Middenstand en Energie).

Received: ((will be filled in by the editorial staff))
Revised: ((will be filled in by the editorial staff))
Published online: ((will be filled in by the editorial staff))

References

1. Energiewende, A. The European Power Sector in 2017 State of Affairs and Review of Current Developments ANALYSIS *RES-Share of Gross Electricity Generation *.
2. Schalling, A., Arnhold, O., Helfenbein, K., Röpcke, T., and Backhaus, A. (2022) Netzdienliche Wasserstofferzeugung.
3. Portuguese government confirms world record solar price of $0.01316/kWh – pv magazine International. *https://www.pv-magazine.com/2020/08/27/portuguese-government-confirms-world-record-solar-price-of-0-01316-kwh/*.
4. Global Hydrogen Trade to Meet the 1.5°C Climate Goal: Trade Outlook for 2050 and Way Forward. */publications/2022/Jul/Global-Hydrogen-Trade-Outlook*.
5. (2020) Clean Hydrogen Partnership - Strategic Research and Innovation Agenda 2021-2027. *https://www.clean-hydrogen.europa.eu/about-us/key-documents/strategic-research-and-innovation-agenda_en*.
6. Menezes, M.W., Simmons, D.R., Winberg, S., Baranwal, R., Hoffman, P., and Genatowski, S.L. U.S. Department of Energy Hydrogen Program Plan.
7. EY, imec, RINA, C. (2020) Study on Solar Fuels Research & Invest.
8. Kim, J.H., Hansora, D., Sharma, P., Jang, J.W., and Lee, J.S. (2019) Toward practical solar hydrogen production – an artificial photosynthetic leaf-to-farm challenge. *Chem Soc Rev,* **48** (7), 1908–1971.

9. Andreani, L.C., Bozzola, A., Kowalczewski, P., Liscidini, M., and Redorici, L. (2018) Silicon solar cells: toward the efficiency limits. *https://doi.org/10.1080/23746149.2018.1548305*, **4** (1), 1548305.

10. Hermle, M., Feldmann, F., Bivour, M., Goldschmidt, J.C., and Glunz, S.W. (2020) Passivating contacts and tandem concepts: Approaches for the highest silicon-based solar cell efficiencies. *Appl Phys Rev*, **7** (2), 021305.

11. Ho-Baillie, A.W.Y., Zheng, J., and Mahmud, A. (2021) Recent progress and future prospects of perovskite tandem solar cells COLLECTIONS ARTICLES YOU MAY BE INTERESTED IN. *Cite as: Appl. Phys. Rev*, **8**, 41307.

12. IRENA, International Renewable Energy Agency, A.Dhabi. (2020) Green Hydrogen Cost Reduction: Scaling up Electrolysers to Meet the 1.5^0C Climate Goal. *Report*, 106.

13. Europe, H. (2020) Strategic Research and Innovation Agenda Final Draft.

14. Rongé, J., Bosserez, T., Martel, D., Nervi, C., Boarino, L., Taulelle, F., Decher, G., Bordiga, S., and Martens, J.A. (2014) Monolithic cells for solar fuels. *Chem Soc Rev*, **43** (23), 7963–7981.

15. Ager, J.W., Shaner, M.R., Walczak, K.A., Sharp, I.D., and Ardo, S. (2015) Experimental demonstrations of spontaneous, solar-driven photoelectrochemical water splitting. *Energy Environ Sci*, **8** (10), 2811–2824.

16. Tembhurne, S., Nandjou, F., and Haussener, S. (2019) A thermally synergistic photo-electrochemical hydrogen generator operating under concentrated solar irradiation. *Nature Energy 2019 4:5*, **4** (5), 399–407.

17. Kemppainen, E., Aschbrenner, S., Bao, F., Luxa, A., Schary, C., Bors, R., Janke, S., Dorbandt, I., Stannowski, B., Schlatmann, R., and Calnan, S. (2020) Effect of the ambient conditions on the operation of a large-area integrated photovoltaic-electrolyser. *Sustain Energy Fuels*, **4** (9), 4831–4847.

18. Calnan, S., Bagacki, R., Bao, F., Dorbandt, I., Kemppainen, E., Schary, C., Schlatmann, R., Leonardi, M., Lombardo, S.A., Milazzo, R.G., Privitera, S.M.S., Bizzarri, F., Connelli, C., Consoli, D., Gerardi, C., Zani, P., Carmo, M., Haas, S., Lee, M., Mueller, M., Zwaygardt, W., Oscarsson, J., Stolt, L., Edoff, M., Edvinsson, T., and Pehlivan, I.B. (2022) Development of

Various Photovoltaic-Driven Water Electrolysis Technologies for Green Solar Hydrogen Generation. *Solar RRL*, **6** (5), 2100479.

19. Schüttauf, J.-W., Modestino, M.A., Chinello, E., Lambelet, D., Delfino, A., Dominé, D., Faes, A., Despeisse, M., Bailat, J., Psaltis, D., Moser, C., and Ballif, C. (2016) Solar-to-Hydrogen Production at 14.2% Efficiency with Silicon Photovoltaics and Earth-Abundant Electrocatalysts. *J Electrochem Soc*, **163** (10), F1177–F1181.

20. Zankowski, S.P., and Vereecken, P.M. (2018) Combining High Porosity with High Surface Area in Flexible Interconnected Nanowire Meshes for Hydrogen Generation and beyond. *ACS Appl Mater Interfaces*, **10** (51), 44634–44644.

21. Zankowski, S.P., and Vereecken, P.M. (2019) Electrochemical Determination of Porosity and Surface Area of Thin Films of Interconnected Nickel Nanowires. *J Electrochem Soc*, **166** (6), D227–D235.

22. Plankensteiner, N., Rupp, R., Steegstra, P., Singh, S., Canto, J.G., Wodarz, S., Blom, M.J.W., John, J., Mees, M., and Vereecken, P.M. (2022) Freestanding µm-thin nanomesh electrodes exceeding 100x current density enhancement for high-throughput electrochemical applications. *Mater Today Energy*, 101172.

23. Van Drunen, J., Kinkead, B., Wang, M.C.P., Sourty, E., Gates, B.D., and Jerkiewicz, G. (2013) Comprehensive structural, surface-chemical and electrochemical characterization of nickel-based metallic foams. *ACS Appl Mater Interfaces*, **5** (14), 6712–6722.

24. Niameh, A., Alhusseny, M., Nasser, A., and Al-Zurfi, N.M.J. (2017) High-Porosity Metal Foams: Potentials, Applications, and Formulations. *Porosity - Process, Technologies and Applications*.

25. Lópezlópez-Fernándezfernández, E., Gil-Rostra, J., Espinósespinós, J.P., Gonzaíez-Elipe, A.R., De Lucas Consuegra, A., and Yubero, F. (2020) Chemistry and Electrocatalytic Activity of Nanostructured Nickel Electrodes for Water Electrolysis.

26. Machado, S.A.S., and Avaca, L.A. (1994) The hydrogen evolution reaction on nickel surfaces stabilized by H-absorption. *Electrochim Acta*, **39** (10), 1385–1391.

27. Xu, Q., Zhang, L., Zhang, J., Wang, J., Hu, Y., Jiang, H., and Li, C. (2022) EnergyChem 4 (2022) 100087 Available online 4.

28. Lee, S.A., Kim, J., Kwon, K.C., Park, S.H., and Jang, H.W. (2022) Anion exchange membrane water electrolysis for sustainable large-scale hydrogen production. *Carbon Neutralization*, **1** (1), 26–48.

29. Rodriguez, C.A., Modestino, M.A., Psaltis, D., and Moser, C. (2014) Design and cost considerations for practical solar-hydrogen generators. *Energy Environ Sci*, **7** (12), 3828–3835.

30. Beaucarne, G. (2016) Materials Challenge for Shingled Cells Interconnection. *Energy Procedia*, **98**, 115–124.

31. Cox, C.R., Lee, J.Z., Nocera, D.G., and Buonassisi, T. (2014) Ten-percent solar-to-fuel conversion with nonprecious materials. *Proc Natl Acad Sci U S A*, **111** (39), 14057–14061.

32. Li, J., Wang, Y., Zhou, T., Zhang, H., Sun, X., Tang, J., Zhang, L., Al-Enizi, A.M., Yang, Z., and Zheng, G. (2015) Nanoparticle Superlattices as Efficient Bifunctional Electrocatalysts for Water Splitting. *J Am Chem Soc*, **137** (45), 14305–14312.

33. Landman, A., Dotan, H., Shter, G.E., Wullenkord, M., Houaijia, A., Maljusch, A., Grader, G.S., and Rothschild, A. (2017) Photoelectrochemical water splitting in separate oxygen and hydrogen cells. *Nature Materials 2017 16:6*, **16** (6), 646–651.

34. Xin, Y., Kan, X., Gan, L.Y., and Zhang, Z. (2017) Heterogeneous Bimetallic Phosphide/Sulfide Nanocomposite for Efficient Solar-Energy-Driven Overall Water Splitting. *ACS Nano*, **11** (10), 10303–10312.

35. Heremans, G., Trompoukis, C., Daems, N., Bosserez, T., Vankelecom, I.F.J., Martens, J.A., and Rongé, J. (2017) Vapor-fed solar hydrogen production exceeding 15% efficiency using earth abundant catalysts and anion exchange membrane. *Sustain Energy Fuels*, **1** (10), 2061–2065.

36. Chen, H., Song, L., Ouyang, S., Wang, J., Lv, J., and Ye, J. (2019) Co and Fe Codoped WO2.72 as Alkaline-Solution-Available Oxygen Evolution Reaction Catalyst to Construct Photovoltaic Water Splitting System with Solar-To-Hydrogen Efficiency of 16.9%. *Advanced Science*, **6** (16), 1900465.

37. Pehlivan, İ.B., Oscarsson, J., Qiu, Z., Stolt, L., Edoff, M., and Edvinsson, T. (2021) NiMoV and NiO-based catalysts for efficient solar-driven water splitting using thermally integrated photovoltaics in a scalable approach. *iScience*, **24** (1), 101910.

38. Chen, Y., Rui, K., Zhu, J., Dou, S.X., and Sun, W. (2019) Recent Progress on Nickel-Based Oxide/(Oxy)Hydroxide Electrocatalysts for the Oxygen Evolution Reaction. *Chemistry - A European Journal*, **25** (3), 703–713.

39. Tsotridis, G. and P. (2021) EU harmonised protocols for testing of low temperature water electrolysers.

40. Alia, S.M., Stariha, S., and Borup, R.L. (2019) Electrolyzer Durability at Low Catalyst Loading and with Dynamic Operation. *J Electrochem Soc*, **166** (15), F1164.

41. Weiß, A., Siebel, A., Bernt, M., Shen, T.-H., Tileli, V., and Gasteiger, H.A. (2019) Impact of Intermittent Operation on Lifetime and Performance of a PEM Water Electrolyzer. *J Electrochem Soc*, **166** (8), F487–F497.

42. Rakousky, C., Reimer, U., Wippermann, K., Kuhri, S., Carmo, M., Lueke, W., and Stolten, D. (2017) Polymer electrolyte membrane water electrolysis: Restraining degradation in the presence of fluctuating power. *J Power Sources*, **342**, 38–47.

43. Kojima, H., Nagasawa, K., Todoroki, N., Ito, Y., Matsui, T., and Nakajima, R. (2023) Influence of renewable energy power fluctuations on water electrolysis for green hydrogen production. *Int J Hydrogen Energy*, **48** (12), 4572–4593.

44. Uchino, Y., Kobayashi, T., Hasegawa, S., Nagashima, I., Sunada, Y., Manabe, A., Nishiki, Y., and Mitsushima, S. (2018) Dependence of the Reverse Current on the Surface of Electrode Placed on a Bipolar Plate in an Alkaline Water Electrolyzer. *Electrochemistry*, **86** (3), 17–00102.

45. (2020) HighLite project. *https://www.highlite-h2020.eu/*.

Table of contents entry - text

This work presents a PV-EC system combining shingled standard-sized silicon PV and anion-exchange membrane water electrolysis with high surface area electrodes. During >20h operation the system provides a stable η_{STH} of 10% determined through in-situ monitoring of the H_2 flow, operating current/voltage. Best practices for the η_{STH} determination are discussed and benchmarked towards important parameters for practical device implementation.